



Article type: A-Regular research paper

# Real Solar Cell and Determination Methods of Electrical Parameters

**E.M. Keita, F. Mbaye, M. Dia, C. Sow, C. Sene, B. Mbow**

Laboratoire des Semiconducteurs et d'Énergie Solaire, Département de Physique, Faculté des Sciences et Techniques, Université Cheikh Anta Diop, Dakar, Sénégal

Corresponding author : [elouazy@hotmail.fr](mailto:elouazy@hotmail.fr)

RECEIVED: 02 January 2023 / RECEIVED IN FINAL FORM: 21 April 2023 / ACCEPTED: 08 May 2023

**Abstract :** In this work, we develop methods to determine the characteristic electrical parameters of a photovoltaic cell such as the photocurrent density ( $J_{ph}$ ), the saturation current density ( $J_0$ ), the short-circuit current density ( $J_{sc}$ ), the open-circuit voltage ( $V_{oc}$ ), the maximum power density point ( $J_m$ ,  $V_m$ ), the fill factor (FF) and the electrical conversion efficiency ( $\eta_c$ ) according to the irradiance spectrum. The real solar cell model is considered for the determination of these various parameters. This model takes into account the effect of shunt and series resistances (parasitic resistances). Notions of semiconductor physics, continuity equation of charge carriers combined to optoelectronic and geometrical properties of the materials, numerical resolution method to solve implicit equations based on characteristic equation of a photodiode, are notions mainly exploited to determine electrical parameters of the real solar cell. The results are applied to the heterostructures  $ZnO(n^+)/CdS(n)/CuInS_2(p)/CuInSe_2(p^+)$  named CIS and  $ZnO(n^+)/CdS(n)/CuInSe_2(p)/CuInS_2(p^+)$  named CISE to evaluate their performances according to the considered parameters. The results obtained for each structure, photocurrent density  $\sim 17 \text{ mA}\cdot\text{cm}^{-2}$  (CIS) and  $31 \text{ mA}\cdot\text{cm}^{-2}$  (CISE), short-circuit current density  $\sim 16.79 - 17 \text{ mA}\cdot\text{cm}^{-2}$  (CIS) and  $30.62 - 31 \text{ mA}\cdot\text{cm}^{-2}$  (CISE), open-circuit voltage  $\sim 0.76 \text{ V}$  (CIS) and  $0.52 \text{ V}$  (CISE), fill factor  $\sim 0.648 - 0.745$  (CIS) and  $0.545 - 0.677$  (CISE), maximum power density  $\sim 8.28 - 9.69 \text{ mW}\cdot\text{cm}^{-2}$  (CIS) and  $8.72 - 11.02 \text{ mW}\cdot\text{cm}^{-2}$  (CISE), saturation current  $\sim 4.117 \times 10^{-8} \text{ mA}\cdot\text{cm}^{-2}$  (CIS) and  $1.169 \times 10^{-3} \text{ mA}\cdot\text{cm}^{-2}$  (CISE), are in the same magnitude order as the values published in the literature. We obtain under AM 1.5 solar spectrum and taken into account the parasitic resistances, a theoretical conversion efficiency ranging from 9.93% to 11.62% for the model CIS and from 10.46% to 13.22% for the model CISE. Thus, these results allow to validate the various models established to model the phenomena studied.

**Keywords :** Real Solar Cell, Electrical Parameters, Conversion Efficiency

Cite this article: E.M. Keita, F. Mbaye, M. Dia, C. Sow, C. Sene, B. Mbow, *OAJ Materials and Devices*, Vol 7, 0106 - 1 (2023) – DOI: 10.23647/ca.md20230106

# 1. Introduction

The determination of the electrical parameters is particularly important for estimating the performance of a solar cell, in particular the electrical conversion efficiency. Usually the photodiode model is used to model the operation of a solar cell. The solar cell (in the case of inorganic materials) is a photodiode that operates without external bias and delivers its photocurrent through a load. Without illumination (in dark condition), the photodiode behaves like a conventional diode and obeys Schokley's relation [1].

We distinguish the model of the ideal solar cell and that of the real solar cell. For the latter, the losses due to the presence of parasitic resistances in the materials which form the device, is taken into account. The model of the ideal solar cell presents an analytical resolution allowing to determine easily some of the characteristic parameters of the solar cell. The real solar cell model exhibits a current - voltage characteristic described by an implicit relation, it does not admit analytical resolution. We used a resolution method based on approximate calculation techniques (graphical or numerical resolution method) to easily find the different parameters that model the real case of the photodiode. These methods allow to determine from equivalent model equation of the solar cell, the electrical parameters such as: the saturation current density ( $J_0$ ), the short-circuit current density ( $J_{sc}$ ), the open-circuit voltage ( $V_{oc}$ ), the maximum power density point ( $J_m, V_m$ ) and the fill factor (FF).

The determination of the saturation current is based on fundamental notions of semiconductor physics, the assumptions of quasi Fermi level and Schokley-Read will be exploited for the determination of this parameter and the dark current (under external bias). We will consider the regime of low injections of carriers.

## 2. Theory and method

### 2-1. Characteristic equation of a photodiode

Without illumination, a photodiode operates like a conventional diode and obeys Schokley's relation [1]:

$$J_v = -J_0 \cdot \left( e^{qV_j/\eta KT} - 1 \right) \tag{1}$$

$J_0$  is the saturation current density of the photodiode,  $K$  is the Boltzmann constant,  $\eta$  is the ideality factor,  $T$  is the temperature. Under illumination, we take into account the photo-generated current density  $J_{ph}$  and obtain:

$$J = J_{ph} + J_v = J_{ph} - J_0 \cdot \left( e^{qV_j/\eta KT} - 1 \right) \tag{2}$$

$J_{ph}$  is the current density generated by the illumination, its expression is given by [2, 3] :

$$J_{ph} = \int_1^4 qF(1-R)S_{rp} dE \approx \frac{\delta E}{2} [J_{rp}(E_1) + J_{rp}(E_{m+1}) + 2 \sum_{i=2}^m J_{rp}(E_i)] \tag{3}$$

With :  $E \in [1 eV, 4 eV]$ ;  $E_1 = 1 eV$ ;  $E_{m+1} = 4 eV$ ;  $\delta E = \frac{E_{m+1} - E_1}{m}$  (eV)

$E_{i+1} = E_1 + i \cdot \delta E$  (eV) with :  $i : 1 \dots m$

In the case of a 4-layer structure type n+pp+, the spectral response  $S_{rp}$  is given by [4]:

$$S_{rp} = \frac{J_{p1} + J_{p2} + J_w + J_{n1} + J_{n2}}{qF(1-R)} \tag{4}$$

The expressions of photocurrent densities  $J_{p1}, J_{p2}, J_w, J_{n1}, J_{n2}$  of minority carriers are given in the appendix.

$$J_{rp} = qF(1-R)S_{rp} \tag{5}$$

$$F = \Phi \times \frac{1.24}{E^2} \tag{6}$$

$$J_{rp} = q \times \Phi \times \frac{1.24}{E^2} (1-R)S_{rp} \tag{7}$$

$$EQE = (1-R)S_{rp} \tag{8}$$

$\Phi$  represents the flux of photons versus the wavelength, it is expressed in  $cm^{-2} \cdot s^{-1} \cdot \mu m^{-1}$ .  $F$  is the flux of photons versus the energy, it expressed in  $cm^{-2} \cdot s^{-1} \cdot eV^{-1}$  [3]. EQE is the external quantum efficiency and  $S_{rp}$  is the internal quantum efficiency or spectral response.  $R$  is the reflection coefficient of the frontal layer.  $J$  is the current density supplied by the photodiode,  $V_j$  is the bias voltage across the n/p junction. The voltage  $V_j$  can be expressed as a function of the bias voltage  $V$  which appears at the terminals of the load supplied by the solar cell.

### 2-2. Real solar cell

In the case of a real solar cell, it is take into account the ohmic voltage drops within the layers of materials which constitute the cell, modeled by a series resistance  $R_s$  and current losses modeled by a shunt resistance  $R_{sh}$ . In the model of the real solar cell, we have :

$$V_j = V + R_s \cdot J \tag{9}$$

The characteristic equation of the solar cell is given by :

$$J = J_{ph} - J_0 \left( e^{\frac{q(V+R_s J)}{\eta KT}} - 1 \right) - \frac{V+R_s J}{R_{sh}} \tag{10}$$

The corresponding electrical diagram is shown in figure 1.

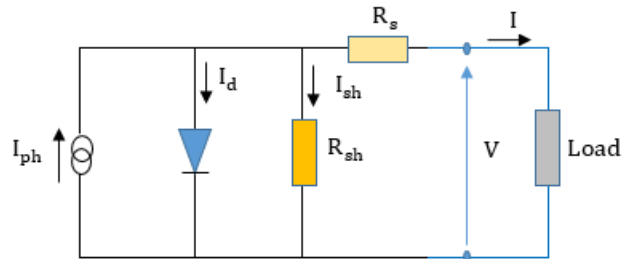


Figure 1 : Equivalent electrical diagram of a real solar cell

### 2-2-1. Determination of the saturation current

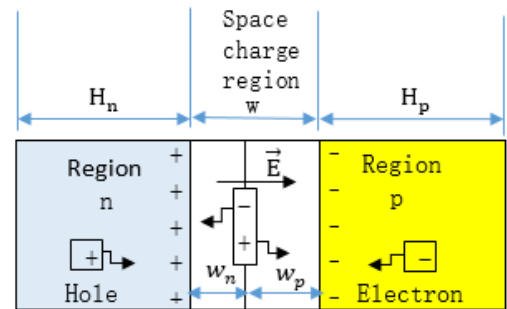


Figure 2 : Junction n/p diagram

The determination of the saturation current is based on fundamental notions of semiconductor physics and using the continuity equation, the assumptions of quasi Fermi level and Shockley-Read are exploited for the determination of this parameter and of the dark current (under external bias voltage) [5, 6]. We consider the regime of low injections of carriers. The n/p junction diagram is shown in figure 2.

$$\frac{\partial n}{\partial t} = \frac{1}{q} \text{div} \vec{J}_n + g_n - r_n \quad (11)$$

$$\frac{\partial p}{\partial t} = -\frac{1}{q} \text{div} \vec{J}_p + g_p - r_p \quad (12)$$

With :  $\vec{J}_n = qn\mu_n \vec{E} + qD_n \cdot \overrightarrow{\text{grad}}(n)$  (13)

$$\vec{J}_p = qp\mu_p \vec{E} - qD_p \cdot \overrightarrow{\text{grad}}(p) \quad (14)$$

For a stationary regime we have :

$$\frac{\partial n}{\partial t} = \frac{\partial p}{\partial t} = 0 \quad (15)$$

The expression of saturation current density  $J_0$  can be written as:

$$J_0 = \frac{qD_n}{L_n} \left[ \frac{\text{ch}\left(\frac{H_p}{L_n}\right)}{\text{sh}\left(\frac{H_p}{L_n}\right)} \right] \cdot \frac{n_{ip}^2}{N_{ap}} + \frac{qD_p}{L_p} \left[ \frac{\text{ch}\left(\frac{H_n}{L_p}\right)}{\text{sh}\left(\frac{H_n}{L_p}\right)} \right] \cdot \frac{n_{in}^2}{N_{dn}} + J_{rg} \quad (16)$$

$J_{rg}$  is the recombination current in the space charge area, it is written as :

$$J_{rg} = \left( q \times \frac{1}{\tau_n} \frac{n_{in}}{2} \times W_n + q \times \frac{1}{\tau_p} \frac{n_{ip}}{2} \times W_p \right) \quad (17)$$

With :  $n_{in} = (N_{cn} \cdot N_{vn})^{\frac{1}{2}} \cdot e^{-\frac{E_{gn}}{2 \cdot k \cdot T}}$  (18)

$$n_{ip} = (N_{cp} \cdot N_{vp})^{\frac{1}{2}} \cdot e^{-\frac{E_{gp}}{2 \cdot k \cdot T}} \quad (19)$$

$$kT \ln \left( \frac{n_{ip}^2}{N_{ap} N_{dn}} \frac{N_{cn}}{N_{cp}} \right) = -q(\chi_n - \chi_p) - q \cdot V_d \quad (20)$$

For a n/p heterojunction structure, the diffusion voltage  $V_d$  or potential barrier at the junction can be written as:

$$V_d = \frac{E_{gp} + E_{gn}}{2q} - \left[ \frac{\Delta E_g}{2q} + \Delta\chi + \frac{kT}{q} \ln \left( \frac{N_{cn} N_{vp}}{N_{dn} N_{ap}} \right) \right] \quad (21)$$

With :  $\Delta E_g = E_{gn} - E_{gp}$  (22)

$$\Delta\chi = \chi_n - \chi_p \quad (23)$$

The thicknesses of the n and p regions of the space charge region ( $W_n$  and  $W_p$ ), can be respectively written as [5]:

$$W_n \approx \left( \frac{2 N_{ap}}{q N_{dn}} \cdot \frac{\epsilon_n \cdot \epsilon_p}{\epsilon_n N_{dn} + \epsilon_p N_{ap}} \cdot V_d \right)^{\frac{1}{2}} \quad (24)$$

$$W_p \approx \left( \frac{2 N_{dn}}{q N_{ap}} \cdot \frac{\epsilon_n \cdot \epsilon_p}{\epsilon_n N_{dn} + \epsilon_p N_{ap}} \cdot V_d \right)^{\frac{1}{2}} \quad (25)$$

The various parameters used are defined in the nomenclature.

### 2-2-2. Short-circuit current density $J_{sc}$

For a real solar cell modeled by equation (10), the short-circuit current density is given by the following implicit relation:

$$J_{sc} = \frac{\eta KT}{q R_s} \cdot \ln \left( \frac{J_{ph}}{J_0} - \frac{J_{sc}}{J_0} - \frac{R_s J_{sc}}{R_{sh} J_0} + 1 \right) \quad (26)$$

The short-circuit current density therefore depends on the shunt and series resistances.

### 2-2-3. Open circuit voltage $V_{oc}$

The open-circuit voltage obeys the following implicit relation:

$$V_{oc} = \frac{\eta KT}{q} \ln \left( \frac{J_{ph}}{J_0} - \frac{V_{oc}}{R_{sh} J_0} + 1 \right) \quad (27)$$

It does not depend on the series resistance.

### 2-2-4. Maximum power density point

The electrical power density is defined by the relation:

$$P = J \cdot V \quad (28)$$

Where  $J$  is the current density supplied by the solar cell and  $V$  the bias voltage at its terminals. We obtain :

$$\frac{\partial P}{\partial V} = V \frac{\partial J}{\partial V} + J \quad (29)$$

We have :  $J = J_{ph} - J_0 \left( e^{\frac{q(V+R_s J)}{\eta KT}} - 1 \right) - \frac{V+R_s J}{R_{sh}}$  (30)

So we can write :

$$\frac{\partial J}{\partial V} = -J_0 \frac{\partial}{\partial V} \left( \frac{q(V+R_s J)}{\eta KT} \right) e^{\frac{q(V+R_s J)}{\eta KT}} - \frac{\partial}{\partial V} \left( \frac{V+R_s J}{R_{sh}} \right) \quad (31)$$

We obtain :

$$\frac{\partial J}{\partial V} = -J_0 \frac{q}{\eta KT} \left( \frac{\partial V}{\partial V} + R_s \frac{\partial J}{\partial V} \right) e^{\frac{q(V+R_s J)}{\eta KT}} - \frac{1}{R_{sh}} \frac{\partial V}{\partial V} - \frac{R_s}{R_{sh}} \frac{\partial J}{\partial V} \quad (32)$$

In equation (32), by factorising by  $\frac{\partial J}{\partial V}$  and noticing that  $\frac{\partial V}{\partial V} = 1$ , we obtain :

$$\frac{\partial J}{\partial V} \left( 1 + \frac{q J_0 R_s}{\eta KT} e^{\frac{q(V+R_s J)}{\eta KT}} + \frac{R_s}{R_{sh}} \right) = -\frac{\partial V}{\partial V} \left( \frac{q J_0}{\eta KT} e^{\frac{q(V+R_s J)}{\eta KT}} + \frac{1}{R_{sh}} \right) \quad (33)$$

From equation (33) we can determine the expression of  $\frac{\partial J}{\partial V}$ , we obtain :

$$\text{We obtain : } \frac{\partial J}{\partial V} = -\frac{\frac{q J_0}{\eta KT} e^{\frac{q(V+R_s J)}{\eta KT}} + \frac{1}{R_{sh}}}{1 + \frac{q J_0 R_s}{\eta KT} e^{\frac{q(V+R_s J)}{\eta KT}} + \frac{R_s}{R_{sh}}} \quad (34)$$

At the maximum power density point, we can write :

$$\frac{\partial P}{\partial V} = V \frac{\partial J}{\partial V} + J = 0 \quad (35)$$

We obtain the relation :

$$J - \frac{\frac{q V J_0}{\eta K T} e^{\frac{q(V+R_s J)}{\eta K T}} + \frac{V}{R_{sh}}}{1 + \frac{q J_0 R_s}{\eta K T} e^{\frac{q(V+R_s J)}{\eta K T}} + \frac{R_s}{R_{sh}}} = 0 \quad (36)$$

However, the solution of relation (36) must verify equation (30) which models the real solar cell, so the current density  $J_m$  and the voltage  $V_m$  at the maximum power density point  $P_m$  must verify the following equation system :

$$\begin{cases} J - \frac{\frac{q V J_0}{\eta K T} e^{\frac{q(V+R_s J)}{\eta K T}} + \frac{V}{R_{sh}}}{1 + \frac{q J_0 R_s}{\eta K T} e^{\frac{q(V+R_s J)}{\eta K T}} + \frac{R_s}{R_{sh}}} = 0 \\ J = J_{ph} - J_0 \left( e^{\frac{q(V+R_s J)}{\eta K T}} - 1 \right) - \frac{V+R_s J}{R_{sh}} \end{cases} \quad (37)$$

Approximate solving techniques are used to solve the various implicit equations. Considering that the space charge zone is located only between the n and p regions and that the electric field is zero outside this zone, the results obtained can be applied to the heterojunctions ZnO(n<sup>+</sup>)/CdS(n)/CuInS<sub>2</sub>(p)/CuInSe<sub>2</sub>(p<sup>+</sup>) and ZnO(n<sup>+</sup>)/CdS(n)/CuInSe<sub>2</sub>(p)/CuInS<sub>2</sub>(p<sup>+</sup>) to evaluate their performance and compare them to those published in the literature.

### 2-2-5. Electrical conversion efficiency ( $\eta_c$ )

The electrical conversion efficiency of the photovoltaic cells  $\eta_c$  is defined as the ratio between the maximum power delivered by the cell  $P_m^*$  and the incident solar power  $P_{solar}$ , it is given by:

$$\eta_c = \frac{P_m^*}{P_{solar}} = \frac{P_m}{S_r} = \frac{FF \times V_{oc} \times I_{sc}}{S_r \times A_s} = \frac{FF \times V_{oc} \times J_{sc}}{S_r} \quad (38)$$

With :

$$FF = \frac{P_m^*}{I_{sc} \cdot V_{oc}} = \frac{P_m}{I_{sc} \cdot V_{oc}} \quad (39)$$

$$P_{solar} = S_r \times A_s \quad (40)$$

$$I_{sc} = J_{sc} \times A_s \quad (41)$$

$FF$  is the fill factor and  $S_r$  is the solar radiation (W/m<sup>2</sup>),  $S_r = 1000$  W/m<sup>2</sup> under standard conditions (AM 1.5 G).  $A_s$  is the

active surface of solar panels (m<sup>2</sup>),  $P_m^*$  is the maximum power (W),  $P_m$  is the maximum power density (W/m<sup>2</sup>) and  $I_{sc}$  is the short-circuit current (A).

### 2-2-6. Method and technique of resolution

The established implicit equations do not admit an analytical solution but they can be solved using a graphical method or a numerical method of resolution (approximate calculation). To solve these equations in order to have access to the characteristic parameters of the solar cell, we mainly used a numerical method of resolution and particularly the secant method [7]. It will be a question of using an iterative resolution method which is based on the following principle :

- first we initialize with the data of two values  $x_0$  and  $x_1$  which must surround the solution;
- and then we proceed to the following iterative resolution:

$$x_{n+1} = x_n - \frac{f(x_n) [x_n - x_{n-1}]}{f(x_n) - f(x_{n-1})} \quad (42)$$

By getting closer to the solution of the problem,  $x_{n+1}$  tends towards  $x_n$  and the solutions are quasi-stationary, and therefore we can impose a shutoff parameter  $\xi$  defined by :

$$|x_{n+1} - x_n| < \xi \quad (43)$$

However for the system of equations (37) allowing to determine the maximum power point, we first do a graphic resolution to locate the solution, then among the different solutions of equation (30) obtained by the secant method, we check among the pairs of solutions ( $J, V$ ), the one who verifies the equation (36) up to a given precision.

## 3. Results and discussion

In this part we apply the established results to plot the current density - voltage characteristic noted  $J$  (V) ( $J$  is the current density supplied by the solar cell and  $V$  the voltage at its terminals) and determine theoretically the characteristic of electrical parameters of solar cells in the case of a heterojunction: ZnO (n<sup>+</sup>)/CdS (n)/CuInS<sub>2</sub> (p)/CuInSe<sub>2</sub> (p<sup>+</sup>) and ZnO (n<sup>+</sup>)/CdS (n)/CuInSe<sub>2</sub> (p)/CuInS<sub>2</sub> (p<sup>+</sup>).

**Table 1. Data of used parameters**

Material	$N_v$ (cm <sup>-3</sup> )	$N_c$ (cm <sup>-3</sup> )	$E_g$ (eV)	$\chi$ (eV)	$\tau_n, \tau_p$ (s)	$\epsilon$	$N_d, N_a$ (cm <sup>-3</sup> )
CdS	$5 \cdot 10^{19}$	$1 \cdot 10^{19}$	2.35	4.4	$10^{-8}$	$10 \cdot \epsilon_0$	$7.6 \cdot 10^{17}$
CuInS <sub>2</sub>	$2 \cdot 10^{19}$	$5 \cdot 10^{18}$	1.57	4.04	$10^{-8}$	$15 \cdot \epsilon_0$	$1.9 \cdot 10^{17}$
CuInSe <sub>2</sub>	$2 \cdot 10^{19}$	$5 \cdot 10^{18}$	1.04	4.58	$10^{-8}$	$15 \cdot \epsilon_0$	$1.9 \cdot 10^{17}$

**Table 2. Results obtained**

Junction	$J_0$ (mA · cm <sup>-2</sup> )	$V_d$ (V)	$W_n$ (μm)	$W_p$ (μm)	$W$ (μm)	$n_{in} - n_{ip}$ (cm <sup>-3</sup> )	$\eta$
CdS/ CuInS <sub>2</sub>	$4.117 \cdot 10^{-8}$	1.023	0.02015	0.08058	0.1007	$4.011 \cdot 10^{-1} - 6.424 \cdot 10^5$	1,5 [8]
CdS/ CuInSe <sub>2</sub>	$1.169 \cdot 10^{-3}$	1.033	0.02024	0.08097	0.1012	$4.011 \cdot 10^{-1} - 1.825 \cdot 10^{10}$	2 [9,10]

$$K = 1.38 \cdot 10^{-23} J \cdot K^{-1}; \epsilon_0 = 8.85418782 \cdot 10^{-12} F \cdot m^{-1}; q = 1.602 \cdot 10^{-19} C; T = 300 K; S_r = 83.4 mW \cdot cm^{-2} \text{ (AM 1,5) [11].}$$

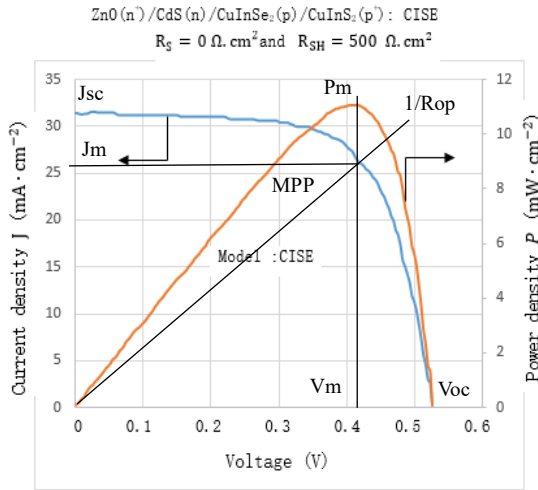


**Figure 3. Evolution of the current density  $J$  and the electrical power density  $P$  versus bias voltage  $V$  for  $R_S = 0 \Omega \cdot \text{cm}^2$  and  $R_{SH} = 500 \Omega \cdot \text{cm}^2$  ( $J_0 = 1.169 \times 10^{-3} \text{ mA} \cdot \text{cm}^{-2}$ ;  $J_{ph} = 31 \text{ mA} \cdot \text{cm}^{-2}$ ;  $\eta = 2$ ). Model  $\text{ZnO}(n^+)/\text{CdS}(n)/\text{CuInS}_2(p)/\text{CuInSe}_2(p^+)$**

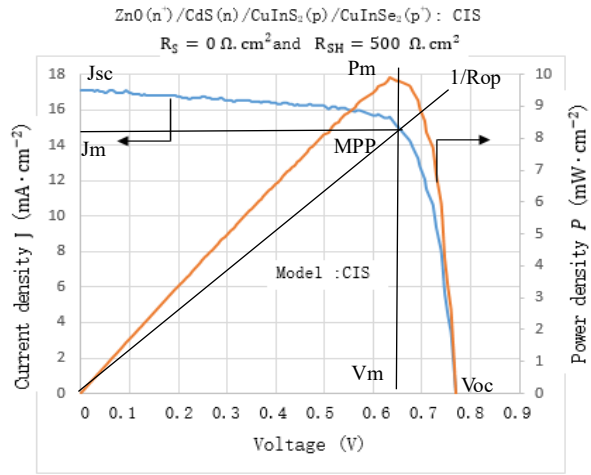


**Figure 4. Evolution of the current density  $J$  and the electrical power density  $P$  versus bias voltage  $V$  for  $R_S = 0 \Omega \cdot \text{cm}^2$  and  $R_{SH} = 500 \Omega \cdot \text{cm}^2$  ( $J_0 = 4.117 \times 10^{-8} \text{ mA} \cdot \text{cm}^{-2}$ ;  $J_{ph} = 17 \text{ mA} \cdot \text{cm}^{-2}$ ;  $\eta = 1.5$ ). Model  $\text{ZnO}(n^+)/\text{CdS}(n)/\text{CuInSe}_2(p)/\text{CuInS}_2(p^+)$**

Table 1 gives the data used to determine the various parameters. From the data in Table 1, we can determine the saturation current density ( $J_0$ ), the diffusion voltage or potential barrier ( $V_d$ ), the thicknesses of the n and p regions of the space charge region ( $W_n$  and  $W_p$ ), and the intrinsic carrier densities ( $n_{in}$  et  $n_{ip}$ ). Regarding the ideality factor ( $\eta$ ), we consider some values taken from the literature [8-10]. The various results obtained are summarized in Table 2. We note that the values of the calculated saturation current density for the two models are in the same magnitude order of those published in the literature [12]. Figures 3 and 4 show

the current-voltage and electrical power-voltage characteristics respectively for the models  $\text{ZnO}(n^+)/\text{CdS}(n)/\text{CuInS}_2(p)/\text{CuInSe}_2(p^+)$  and  $\text{ZnO}(n^+)/\text{CdS}(n)/\text{CuInSe}_2(p)/\text{CuInS}_2(p^+)$  by fixing the series resistance at  $0 \Omega \cdot \text{cm}^2$  and the shunt resistance at  $500 \Omega \cdot \text{cm}^2$ . Each graph combines at the same time the evolution of current and power versus voltage, this allows to graphically determine the maximum power point and the optimal resistance of the load as shown in the figures.

### 3-1. Effect of shunt and series resistances on the current-voltage characteristic

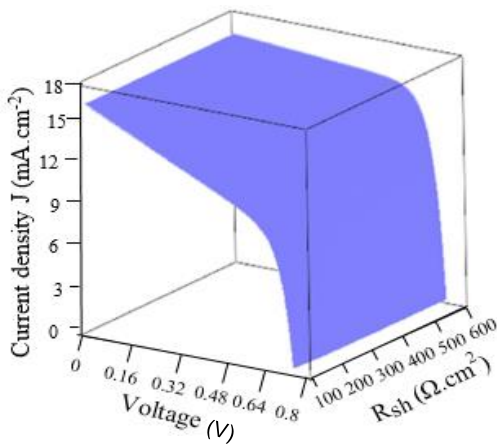


**Figure 5. Three-dimensional representation of current density  $J$  vs. bias voltage  $V$  and shunt resistance  $R_{SH}$  ( $100 \Omega \cdot \text{cm}^2$  to  $600 \Omega \cdot \text{cm}^2$ ) ( $J_0 = 4.117 \cdot 10^{-8} \text{ mA} \cdot \text{cm}^{-2}$ ;  $J_{ph} = 17 \text{ mA} \cdot \text{cm}^{-2}$ ;  $R_S = 0 \Omega \cdot \text{cm}^2$ ;  $\eta = 1.5$ ). Model  $\text{ZnO}(n^+)/\text{CdS}(n)/\text{CuInS}_2(p)/\text{CuInSe}_2(p^+)$**

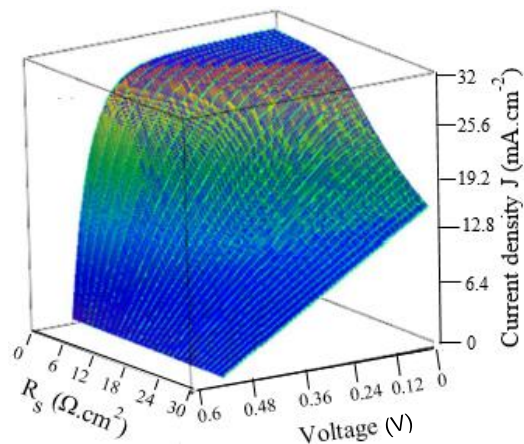


**Figure 6. Three-dimensional representation of current density  $J$  vs. bias voltage  $V$  and series resistance  $R_S$  ( $R_S = 0 \Omega \cdot \text{cm}^2$  to  $30 \Omega \cdot \text{cm}^2$ ) ( $J_0 = 1.169 \cdot 10^{-3} \text{ mA} \cdot \text{cm}^{-2}$ ;  $J_{ph} = 31 \text{ mA} \cdot \text{cm}^{-2}$ ;  $R_{SH} = 600 \Omega \cdot \text{cm}^2$ ;  $\eta = 2$ ). Model  $\text{ZnO}(n^+)/\text{CdS}(n)/\text{CuInS}_2(p)/\text{CuInS}_2(p^+)$**

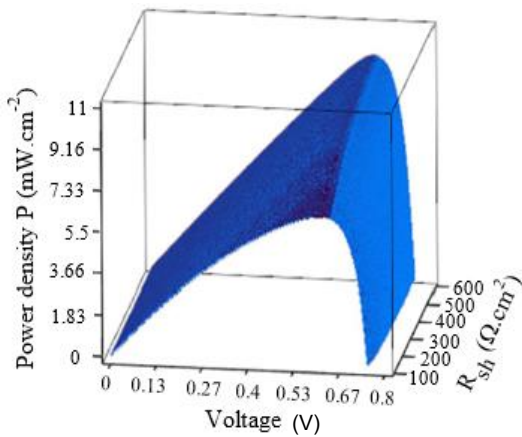


**Figure 7. Three-dimensional representation of electric power density P vs. bias voltage V and shunt resistance  $R_{SH}$  ( $R_{SH} = 100 \Omega \cdot \text{cm}^2$  to  $600 \Omega \cdot \text{cm}^2$ ) ( $J_0 = 4.117 \cdot 10^{-8} \text{ mA} \cdot \text{cm}^{-2}$ ;  $J_{ph} = 17 \text{ mA} \cdot \text{cm}^{-2}$ ;  $R_S = 0 \Omega \cdot \text{cm}^2$ ;  $\eta = 1.5$ ). Model  $\text{ZnO}(n^+)/\text{CdS}(n)/\text{CuInS}_2(p)/\text{CuInSe}_2(p^+)$**

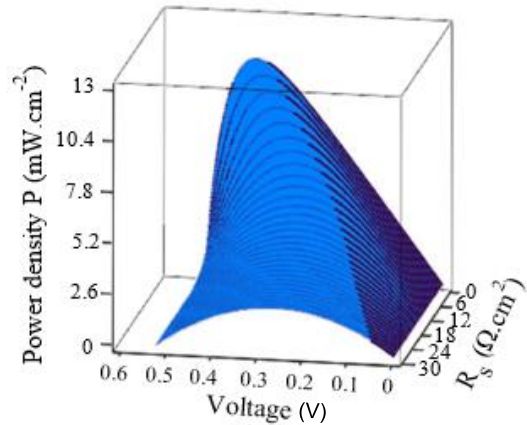


**Figure 8. Three-dimensional representation of electric power density P vs. bias voltage V and series resistance  $R_S$  ( $R_S = 0 \Omega \cdot \text{cm}^2$  to  $30 \Omega \cdot \text{cm}^2$ ) ( $J_0 = 1.169 \cdot 10^{-3} \text{ mA} \cdot \text{cm}^{-2}$ ;  $J_{ph} = 31 \text{ mA} \cdot \text{cm}^{-2}$ ;  $R_{SH} = 600 \Omega \cdot \text{cm}^2$ ;  $\eta = 2$ ). Model  $\text{ZnO}(n^+)/\text{CdS}(n)/\text{CuInSe}_2(p)/\text{CuInS}_2(p^+)$**

In figures 5-8 we represent the current-voltage characteristic for different values of the parasitic resistances, it is a three-dimensional representation which shows the simultaneous evolution of three electrical parameters (J, V, Rs or Rsh). In figures 5 and 7 we highlight the influence of the shunt resistances applied to the model  $\text{ZnO}(n^+)/\text{CdS}(n)/\text{CuInS}_2(p)/\text{CuInSe}_2(p^+)$ , on the evolutions of the current and the electric power according to the voltage respectively. In figures 6 and 8 we study the influence of the series resistances applied to the model  $\text{ZnO}(n^+)/\text{CdS}(n)/\text{CuInSe}_2(p)/\text{CuInS}_2(p^+)$  on the current and the electrical power evolutions according to the voltage respectively. We note that the high values of the series resistance and low

values of the shunt resistance affect the performance of the solar cell, modify the evolution of the J(V) curve and reduce the maximum power of the cell as shown in the figures. These graphs show that the power of the cell increases with a decrease of the series resistance and an increase of the shunt resistance.

**3-2. Comparative study of two models :  $\text{ZnO}(n^+)/\text{CdS}(n)/\text{CuInS}_2(p)/\text{CuInSe}_2(p^+)$  and  $\text{ZnO}(n^+)/\text{CdS}(n)/\text{CuInSe}_2(p)/\text{CuInS}_2(p^+)$**

A comparative study of the two structures is done in figures 9 and 10. The structure where  $\text{CuInS}_2$  is used as the base ( $\text{ZnO}(n^+)/\text{CdS}(n)/\text{CuInS}_2(p)/\text{CuInSe}_2(p^+)$ ) is named CIS and the structure where  $\text{CuInSe}_2$  is used as the base

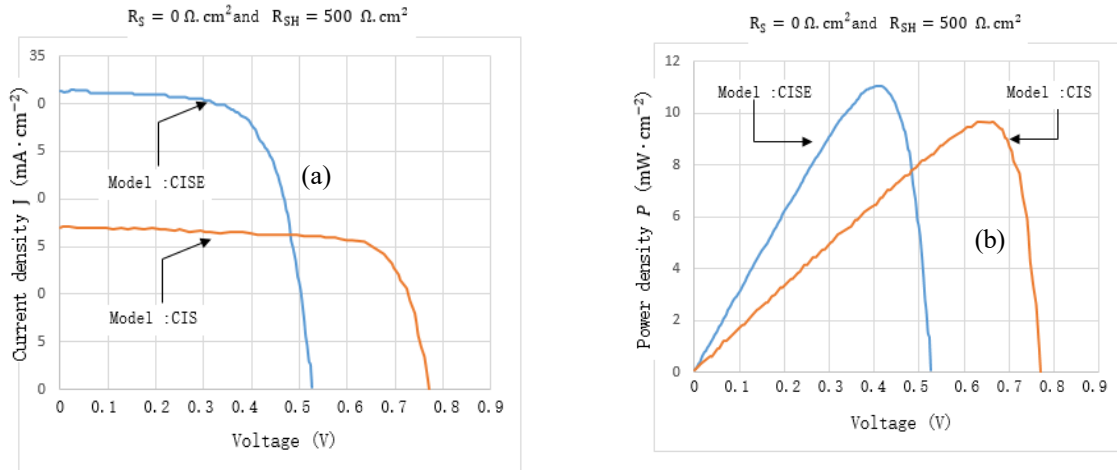


**Figure 9. (a) Comparative study of the evolution of the current density J versus bias voltage V for the two models ; (b) Comparative study of the evolution of the electrical power density P versus bias voltage V for the two models  $R_S = 0 \Omega \cdot \text{cm}^2$  and  $R_{SH} = 500 \Omega \cdot \text{cm}^2$**   
**CISE :  $\text{ZnO}(n^+)/\text{CdS}(n)/\text{CuInSe}_2(p)/\text{CuInS}_2(p^+)$  ( $J_0 = 1.169 \times 10^{-3} \text{ mA} \cdot \text{cm}^{-2}$ ;  $J_{ph} = 31 \text{ mA} \cdot \text{cm}^{-2}$ ;  $\eta = 2$ )**  
**CIS :  $\text{ZnO}(n^+)/\text{CdS}(n)/\text{CuInS}_2(p)/\text{CuInSe}_2(p^+)$  ( $J_0 = 4.117 \times 10^{-8} \text{ mA} \cdot \text{cm}^{-2}$ ;  $J_{ph} = 17 \text{ mA} \cdot \text{cm}^{-2}$ ;  $\eta = 1.5$ )**

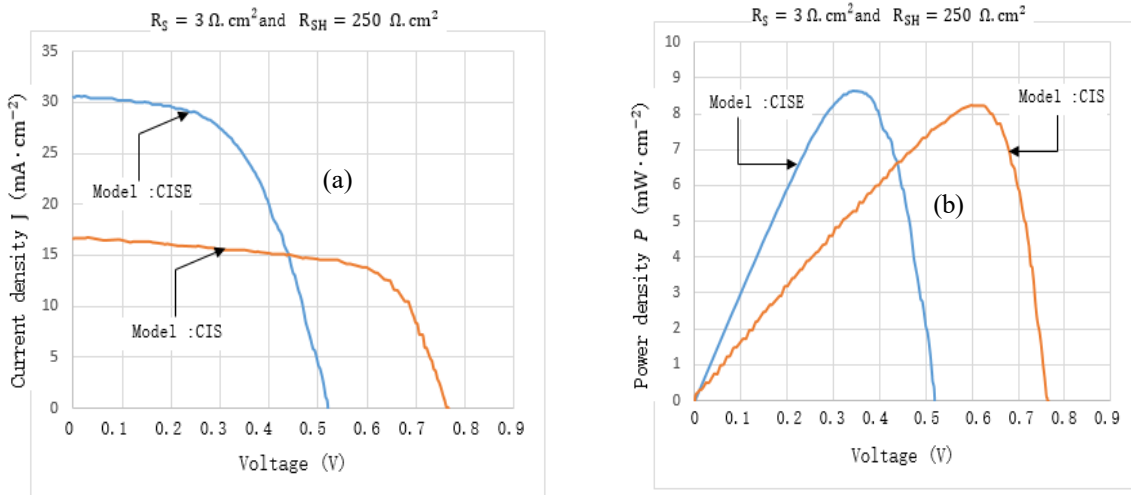


**Figure 10. (a) Comparative study of the evolution of the current density  $J$  versus bias voltage  $V$  for the two models ; (b) Comparative study of the evolution of the electrical power density  $P$  versus bias voltage  $V$  for the two models  $R_S = 3 \Omega.cm^2$  and  $R_{SH} = 250 \Omega.cm^2$**   
**CISE :  $ZnO(n^+)/CdS(n)/CuInSe_2(p)/CuInS_2(p^+)$  ( $J_0 = 1.169 \times 10^{-3} mA \cdot cm^{-2}$ ;  $J_{ph} = 31 mA \cdot cm^{-2}$ ;  $\eta = 2$ )**  
**CIS :  $ZnO(n^+)/CdS(n)/CuInS_2(p)/CuInSe_2(p^+)$  ( $J_0 = 4.117 \times 10^{-8} mA \cdot cm^{-2}$ ;  $J_{ph} = 17 mA \cdot cm^{-2}$ ;  $\eta = 1.5$ )**

( $ZnO(n^+)/CdS(n)/CuInSe_2(p)/CuInS_2(p^+)$ ) is named CISE. We compare the profiles of the current densities  $J$  versus the bias voltage  $V$  (characteristic  $J - V$ ) by fixing the series and shunt resistances at  $R_S = 0 \Omega.cm^2$  and  $R_{SH} = 500 \Omega.cm^2$  in figure 9-a and by fixing  $R_S = 3 \Omega.cm^2$  and  $R_{SH} = 250 \Omega.cm^2$  in figure 10-a. In figures 9-b & 10-b we compare the profiles of the electrical powers  $P$  versus the bias voltage  $V$  resulting from the characteristic  $J - V$  of the two models. To determine the internal quantum efficiency or spectral response  $S_{rp}$  and the current density generated by the illumination  $J_{ph}$  for each model the various parameters considered are indicated in table 4 in the appendix. Figure 12 indicated in appendix, shows the photon fluxes which correspond to the solar spectrum AM1.5 versus the wavelength, it corresponds to irradiation of  $834 W.m^{-2}$  and is adapted from [11, 13], figure 11 shows the definition of solar spectrum AM1.5. It is also represented in the same figure 12 the comparison of the internal quantum efficiency (IQE) of the two models (CISE and CIS) versus the wavelength, it is obtained using equation

(4). We note that the solar cells are sensitive to the spectrum ranging from near infrared to visible. The current density generated by the illumination  $J_{ph}$  (photocurrent density) is determined by numerical method using equations (3 - 8) and the values of tables 4 and 5 in appendix. Table 4 indicates the values of the parameters used for the modeling and table 6 indicates the discretized values of the energy, the wavelength, the photon fluxes and the external quantum efficiency. Table 4 and 6 are indicated in Appendix. For the calculation we obtain the photocurrent density  $J_{ph} = 17 mA.cm^{-2}$  for the structure  $ZnO(n^+)/CdS(n)/CuInS_2(p)/CuInSe_2(p^+)$  (named CIS) and  $J_{ph} = 31 mA.cm^{-2}$  for the structure  $ZnO(n^+)/CdS(n)/CuInSe_2(p)/CuInS_2(p^+)$  (named CISE) indicated in table 5 in appendix. The photocurrent density depends on the parameters considered. The characteristic electrical parameters of each model, resulting from this comparative study are summarized in table 3 respectively for the structures  $ZnO(n^+)/CdS(n)/CuInS_2(p)/CuInSe_2(p^+)$  (named CIS) and  $ZnO(n^+)/CdS(n)/CuInSe_2(p)/CuInS_2(p^+)$  (named CISE).

**Table 3. Characteristic parameters of the solar cell taken from graphs 7 for the two models (CIS and CISE)**

Model	$R_S$ ( $\Omega.cm^2$ )	$R_{SH}$ ( $\Omega.cm^2$ )	$\eta$	$J_m$ ( $mA.cm^{-2}$ )	$V_m$ (V)	$P_m$ ( $mW.cm^{-2}$ )	$R_{optimum}$ ( $\Omega.cm^2$ )	$J_{sc}$ ( $mA.cm^{-2}$ )	$V_{oc}$ (V)	FF	$\eta_c$ (%)
CIS	0	500	1.5	14.889	0.651	9.693	43.723	17	0.765	0.745	11.622
CISE	0	500	2	26.896	0.41	11.027	15.244	31	0.525	0.677	13.222
CIS	3	250	1.5	13.627	0.608	8.285	44.617	16.798	0.761	0.648	9.934
CISE	3	250	2	24.862	0.351	8.726	14.118	30.627	0.523	0.545	10.463

## 4. Conclusion

A method of determining the characteristic parameters of a real photovoltaic cell, such as the saturation current density, the short-circuit current density, the photocurrent density, the open-circuit voltage, the maximum power point, the fill factor has been essentially developed in this paper. The determination of these parameters is particularly important to evaluate the performance of the solar cell, in particular for determining the energy conversion efficiency relative to solar irradiation.

For the determination of these parameters, we are based on notions of semiconductor physics for the determination of the saturation current density and the dark current density, and used an approximate calculation by a numerical resolution method for the determination of the short-circuit current density, the open-circuit voltage and the maximum power point. For the photocurrent density we have exploited the spectral response. The results obtained through the different resolution techniques were applied to heterostructures based on  $\text{CuInS}_2$  and  $\text{CuInSe}_2$  :  $\text{ZnO}(n^+)/\text{CdS}(n)/\text{CuInS}_2(p)/\text{CuInSe}_2(p^+)$  and  $\text{ZnO}(n^+)/\text{CdS}(n)/\text{CuInSe}_2(p)/\text{CuInS}_2(p^+)$ . The case of real solar cell (presence of series and shunt resistances) was mainly considered.

With the  $\text{ZnO}(n^+)/\text{CdS}(n)/\text{CuInS}_2(p)/\text{CuInSe}_2(p^+)$  model named CIS, depending on the used parameters, we obtain a theoretical conversion efficiency of 11.62% and 9.93% under an AM 1.5 solar spectrum. This slightly low efficiency is explained by the low short-circuit current obtained with this model (in order of  $17 \text{ mA.cm}^{-2}$ ) considering the parameters used in table 4 and the presence of series and shunt resistances fixed firstly at  $R_S = 0 \Omega.\text{cm}^2$  and  $R_{SH} = 500 \Omega.\text{cm}^2$ , and secondly at  $R_S = 3 \Omega.\text{cm}^2$  and  $R_{SH} = 250 \Omega.\text{cm}^2$  respectively.

For the  $\text{ZnO}(n^+)/\text{CdS}(n)/\text{CuInSe}_2(p)/\text{CuInS}_2(p^+)$  model named CISE, we obtain a theoretical conversion efficiency of 13.22% and 10.46% under the same solar irradiation conditions according to the used parameters. This slightly low efficiency is explained by the small value of the open-circuit voltage (in order of 0.5 V) due to the relatively low energy band gap of  $\text{CuInSe}_2$  (1.04 eV) and the presence of parasitic resistances taking into account.

However, the results obtained for each model (photocurrent density, short-circuit current density, open-circuit voltage, fill factor, maximum power point, saturation current density) are in agreement and remain within the range of experimental values published in the literature [12], thus allowing to validate the different methods established to model the studied phenomena.

## Nomenclature

### Electrical parameters :

$J_0$  : Saturation current density ( $A.cm^{-2}$ )  
 $J_n$  : Electron current density ( $A.cm^{-2}$ )  
 $J_p$  : Hole current density ( $A.cm^{-2}$ )  
 $g_n, g_p$  : Generation rate of electrons, of holes ( $cm^{-3}.s^{-1}$ )

$r_n, r_p$  : Recombination rate of electrons, of holes ( $cm^{-3}.s^{-1}$ )  
 $\mu_n, \mu_p$  : Mobility of electrons, of holes ( $cm^2.V^{-1}.s^{-1}$ )  
 $n$  : Electron density ( $cm^{-3}$ )  
 $p$  : Hole density ( $cm^{-3}$ )  
 $E$  : Energy (eV)  
 $\vec{E}$  : Electric field ( $V.cm^{-1}$ )  
 $J_{ph}$  : Photocurrent density ( $A.cm^{-2}$ )  
 $J_{sc}$  : Short-circuit current density ( $A.cm^{-2}$ )  
 $V_{oc}$  : Open-circuit voltage (V)  
 $P$  : Maximum power density point ( $W.cm^{-2}$ )  
 $FF$  : Fill factor  
 $\eta$  : Ideality factor  
 $\eta_c$  : Electrical conversion efficiency

### Junction p/n :

$H_n, H_p$  : Thickness of the semiconductor n, p  
 $q \chi_n, q \chi_p$  : Electron affinity of the semiconductor n-type, p-type  
 $E_{gn}, E_{gp}$  : Energy band gap of the semiconductor n, p  
 $N_{cn}, N_{cp}$  : Density of states in the conduction band of the semiconductor n, p  
 $N_{vn}, N_{vp}$  : Density of states in the valence band of the semiconductor n, p  
 $N_{dn}$  : Concentration of the ionized donors in the semiconductor n  
 $N_{ap}$  : Concentration of the ionized acceptors in the semiconductor p  
 $n_{in}, n_{ip}$  : Concentration of intrinsic carriers in the semiconductor n, p  
 $\tau_n, \tau_p$  : Lifetime of the carriers in the space charge region of the semiconductor n, p  
 $\epsilon_n, \epsilon_p$  : Electric permittivity of the semiconductor n, p  
 $D_n$  : Diffusion coefficient of electrons in the p-type semiconductor  
 $L_n$  : Diffusion length of the electrons in the p-type semiconductor  
 $D_p$  : Diffusion coefficient of holes in the n-type semiconductor  
 $L_p$  : Diffusion length of the holes in the n-type semiconductor  
 $W_n, W_p$  : Thickness of the region n, p in the space charge region

### Structure CIS or CISE :

Layer i: Region 1 (ZnO)/ Region 2 (CdS)/ Region 3 ( $\text{CuInS}_2$  or  $\text{CuInSe}_2$ )/ Region 4 ( $\text{CuInS}_2$  or  $\text{CuInSe}_2$ )  
 CIS :  $\text{ZnO}(n^+)/\text{CdS}(n)/\text{CuInS}_2(p)/\text{CuInSe}_2(p^+)$   
 CISE :  $\text{ZnO}(n^+)/\text{CdS}(n)/\text{CuInSe}_2(p)/\text{CuInS}_2(p^+)$   
 $F$  : Incident photons flux ( $cm^{-2}.s^{-1}.eV^{-1}$ )  
 $\Phi$  : Incident photons flux ( $cm^{-2}.s^{-1}.\mu m^{-1}$ )  
 $S_{rp}$  : Spectral response or internal quantum efficiency  
 $\alpha_i$  : Absorption coefficient ( $cm^{-1}$ )  
 $D_{pi}, D_{ni}$  : Diffusion coefficient ( $cm^2.s^{-1}$ )  
 $L_{pi}, L_{ni}$  : Diffusion length ( $\mu m$ )  
 $S_{pi}, S_{ni}$  : Recombination velocity (surface or interface) ( $cm.s^{-1}$ )  
 $J_{pi}, J_{ni}$  : Photocurrent density (holes or electrons) ( $A.cm^{-2}.eV^{-1}$ )

- $H_i$  : Thickness layer  $i$  ( $\mu m$ )
- $R$ : Reflection coefficient of region 1 (ZnO)
- $H$ : Thickness of the structure ( $\mu m$ )
- $w_1$ : Thickness of CdS layer in the space charge region (SCR) ( $\mu m$ )
- $w_2$ : Thickness of CuInSe<sub>2</sub> or CuInS<sub>2</sub> layer in the space charge region (SCR) ( $\mu m$ )
- $w$ : Thickness of the space charge region ( $\mu m$ )
- $J_w$ : Photocurrent density of holes in the space charge region (SCR) ( $A.cm^{-2}.eV^{-1}$ )
- $q$ : Elementary charge ( $1.602 \times 10^{-19}C$ )

**A-2) Table 5. Photocurrent density obtained under AM1.5 solar spectrum**

	CIS	CISE
$J_{ph}$	17 mA.cm <sup>-2</sup>	31 mA.cm <sup>-2</sup>

## Appendix

**A-1) Table 4. Physical parameters considered for the determination of the spectral response and the photocurrent density**

Models CIS & CISE	
$H_1 = 0.3 \mu m$	$H_3 = 1 \mu m$
$L_{p1} = 0.3 \mu m$	$L_{n3} = 3 \mu m$
$S_{p1} = 2 \times 10^7 cm.s^{-1}$	$S_{n3} = 2 \times 10^5 cm.s^{-1}$
$D_{p1} = 0.51 cm^2.s^{-1}$	$D_{n3} = 5.13 cm^2.s^{-1}$
$H_2 = 0.1 \mu m$	$H_4 = 98.5 \mu m$
$L_{p2} = 0.4 \mu m$	$L_{n4} = 1 \mu m$
$S_{p2} = 2 \times 10^5 cm.s^{-1}$	$S_{n4} = 2 \times 10^7 cm.s^{-1}$
$D_{p2} = 0.64 cm^2.s^{-1}$	$D_{n4} = 10.27 cm^2.s^{-1}$
$W_1 = 0.02 \mu m$	$W_2 = 0.08 \mu m$

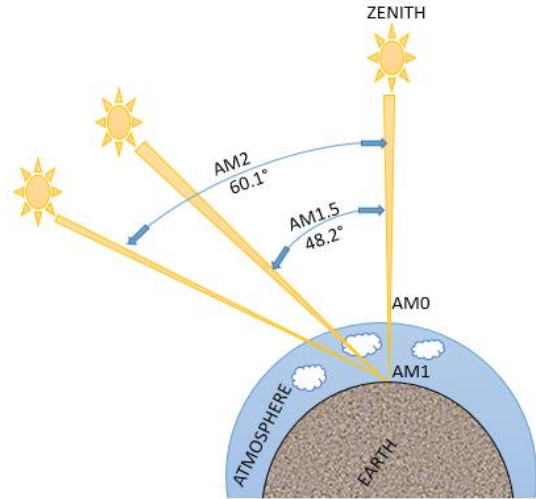


**Figure 11. Definition of the AM standard adapted from [13].**

**A-3) Photocurrent densities of holes and electrons  $J_{p1}$ ,  $J_{p2}$ ,  $J_w$ ,  $J_{n1}$ ,  $J_{n2}$  for a structure n<sup>+</sup>npp<sup>+</sup> [4]**

$$J_{p1} = \frac{q\alpha_1 F(1-R)L_{p1}}{(\alpha_1^2 L_{p1}^2 - 1) \left[ \frac{S_{p2}L_{p2}}{D_{p2}} \text{sh}\left(\frac{H_2}{L_{p2}}\right) + \text{ch}\left(\frac{H_2}{L_{p2}}\right) \right]} \times \left\{ \frac{\left( \frac{S_{p1}L_{p1}}{D_{p1}} + \alpha_1 L_{p1} \right) e^{-\alpha_1 H_1} \left[ \frac{S_{p1}L_{p1}}{D_{p1}} \text{ch}\left(\frac{H_1}{L_{p1}}\right) + \text{sh}\left(\frac{H_1}{L_{p1}}\right) \right]}{\frac{S_{p1}L_{p1}}{D_{p1}} \text{sh}\left(\frac{H_1}{L_{p1}}\right) + \text{ch}\left(\frac{H_1}{L_{p1}}\right)} - \alpha_1 L_{p1} e^{-\alpha_1 H_1} \right\} \quad (A-2)$$

$$J_{p2} = \frac{q\alpha_2 F(1-R)L_{p2} e^{-\alpha_1 H_1}}{(\alpha_2^2 L_{p2}^2 - 1) \left[ \frac{S_{p2}L_{p2}}{D_{p2}} \text{sh}\left(\frac{H_2}{L_{p2}}\right) + \text{ch}\left(\frac{H_2}{L_{p2}}\right) \right]} \times \left\{ \frac{\left( \frac{S_{p2}L_{p2}}{D_{p2}} + \alpha_2 L_{p2} \right) e^{-\alpha_2 H_2} \left[ \frac{S_{p2}L_{p2}}{D_{p2}} \text{ch}\left(\frac{H_2}{L_{p2}}\right) + \text{sh}\left(\frac{H_2}{L_{p2}}\right) \right]}{\frac{S_{p2}L_{p2}}{D_{p2}} \text{sh}\left(\frac{H_2}{L_{p2}}\right) + \text{ch}\left(\frac{H_2}{L_{p2}}\right)} - \alpha_2 L_{p2} e^{-\alpha_2 H_2} \right\} \quad (A-1)$$

$$J_w = -qF(1-R)e^{-\alpha_1 H_1} \left\{ e^{-\alpha_2 H_2} \times [e^{-\alpha_2 w_1} - 1] + e^{-\alpha_2 (H_2 + w_1)} \times [e^{-\alpha_3 w_2} - 1] \right\} \quad (A-3)$$

$$J_{n1} = -\frac{q\alpha_3 L_{n3} F(1-R) e^{[(\alpha_2 - \alpha_1)H_1] + [(\alpha_3 - \alpha_2)(H_1 + H_2 + w_1)]}}{(\alpha_3^2 L_{n3}^2 - 1)} \times \left[ \frac{\left( \alpha_3 L_{n3} - \frac{S_{n3}L_{n3}}{D_{n3}} \right) e^{-\alpha_3 (H_1 + H_2 + w_1)}}{\frac{S_{n3}L_{n3}}{D_{n3}} \text{sh}\left[\frac{H_3}{L_{n3}}\right] + \text{ch}\left[\frac{H_3}{L_{n3}}\right]} + \frac{e^{-\alpha_3 (H_1 + H_2 + w_1)} \left[ \frac{S_{n3}L_{n3}}{D_{n3}} \text{ch}\left(\frac{H_3}{L_{n3}}\right) + \text{sh}\left(\frac{H_3}{L_{n3}}\right) \right]}{\frac{S_{n3}L_{n3}}{D_{n3}} \text{sh}\left[\frac{H_3}{L_{n3}}\right] + \text{ch}\left[\frac{H_3}{L_{n3}}\right]} - \alpha_3 L_{n3} e^{-\alpha_3 (H_1 + H_2 + w_1)} \right] \quad (A-4)$$

$$J_{n2} = - \frac{q \alpha_4 L_{n4} F(1-R) e^{[(\alpha_2 - \alpha_1)H_1]} e^{[(\alpha_3 - \alpha_2)(H_1 + H_2 + w_1)]}}{(\alpha_4^2 L_{n4}^2 - 1) \left\{ \frac{S_{n3} L_{n3}}{D_{n3}} \text{sh} \left[ \frac{H_3}{L_{n3}} \right] + \text{ch} \left[ \frac{H_3}{L_{n3}} \right] \right\}} \times e^{[(\alpha_4 - \alpha_3)(H - H_4)]} \times \left[ \frac{(\alpha_4 L_{n4} - \frac{S_{n4} L_{n4}}{D_{n4}}) e^{-\alpha_4 H}}{\frac{S_{n4} L_{n4}}{D_{n4}} \text{sh} \left( \frac{H_4}{L_{n4}} \right) + \text{ch} \left( \frac{H_4}{L_{n4}} \right)} + \frac{e^{-\alpha_4 (H - H_4)} \left[ \frac{S_{n4} L_{n4}}{D_{n4}} \text{ch} \left( \frac{H_4}{L_{n4}} \right) + \text{sh} \left( \frac{H_4}{L_{n4}} \right) \right]}{\frac{S_{n4} L_{n4}}{D_{n4}} \text{sh} \left( \frac{H_4}{L_{n4}} \right) + \text{ch} \left( \frac{H_4}{L_{n4}} \right)} - \alpha_4 L_{n4} e^{-\alpha_4 (H - H_4)} \right] \quad (A-5)$$

**A-4) Comparative spectral response of CIS and CISE structures and photon flux of AM1.5 solar spectrum**

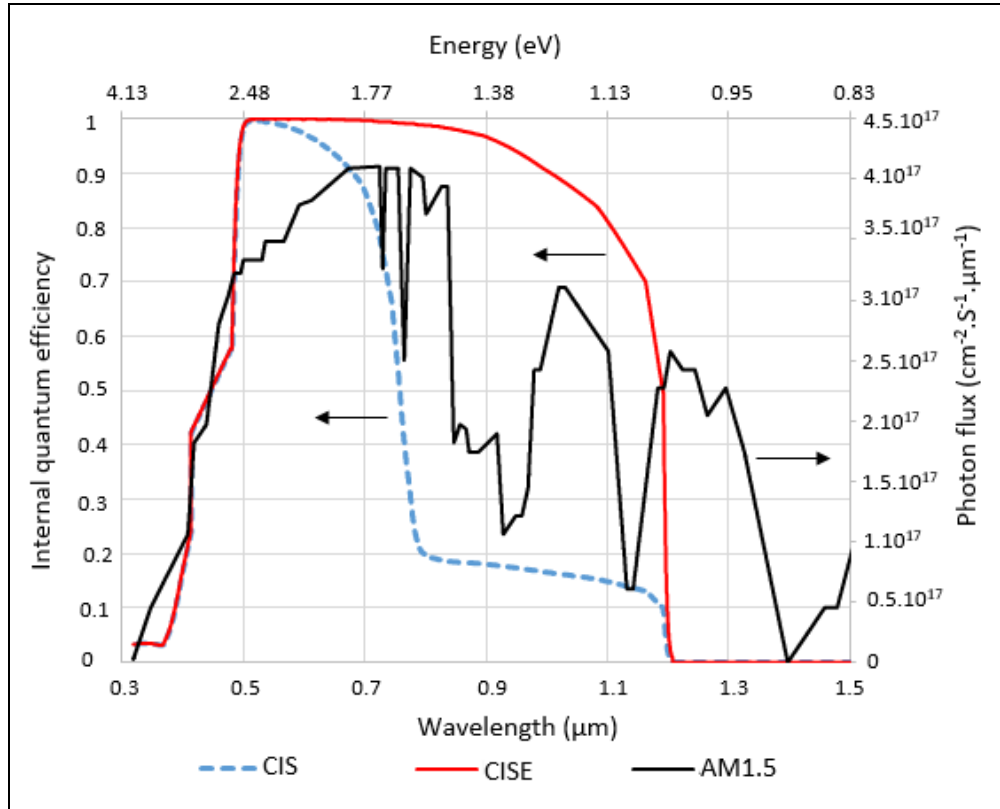


**Figure 12. Internal quantum efficiency (for CIS and CISE structures) and photon flux vs. photon wave length**

**A-5) Table 6. Discretized values of parameters for the calculation of the photocurrent density**

E (eV)	Φ × 10 <sup>17</sup> (cm <sup>2</sup> .s <sup>-1</sup> .μm <sup>-1</sup> )	(1-R)Srp (CISE)	(1-R)Srp (CIS)	Jrg (CISE) (A.cm <sup>-2</sup> .eV <sup>-1</sup> )	Jrp (CIS) (A.cm <sup>-2</sup> .eV <sup>-1</sup> )	E (eV)	Φ × 10 <sup>17</sup> (cm <sup>2</sup> .s <sup>-1</sup> .μm <sup>-1</sup> )	(1-R)Srp (CISE)	(1-R)Srp (CIS)	Jrg (CISE) (A.cm <sup>-2</sup> .eV <sup>-1</sup> )	Jrp (CIS) (A.cm <sup>-2</sup> .eV <sup>-1</sup> )
1	2.424	0	0	0	0	1.54	3.749	0.888	0.175	0.027885	0.005495
1.03	2.57	0.026	0.007	0.001251	0.000336	1.57	4.038	0.889	0.19	0.028930	0.006183
1.06	1.707	0.656	0.125	0.019797	0.003772	1.6	4.011	0.89	0.274	0.027700	0.008528
1.09	0.606	0.748	0.138	0.007579	0.001398	1.63	3.212	0.891	0.407	0.021397	0.009774
1.12	2.247	0.801	0.147	0.028503	0.005231	1.66	4.091	0.891	0.562	0.026277	0.016574
1.15	2.752	0.843	0.154	0.034847	0.006366	1.69	3.933	0.892	0.651	0.024401	0.017808
1.18	2.956	0.867	0.158	0.036563	0.006663	1.72	4.105	0.892	0.716	0.024587	0.019736
1.21	3.106	0.887	0.162	0.037380	0.006827	1.75	4.101	0.893	0.753	0.023755	0.020031
1.24	2.652	0.905	0.166	0.031007	0.005688	1.78	4.098	0.893	0.785	0.022944	0.020169
1.27	2.114	0.923	0.17	0.024032	0.004426	1.81	4.094	0.893	0.801	0.022168	0.019884
1.3	1.212	0.938	0.173	0.013363	0.002465	1.84	4.091	0.893	0.814	0.021435	0.019539
1.33	1.089	0.951	0.176	0.011630	0.002152	1.87	4.046	0.893	0.825	0.020525	0.018962
1.36	1.861	0.962	0.179	0.019228	0.003578	1.9	4.001	0.893	0.834	0.019661	0.018362
1.39	1.764	0.97	0.181	0.017592	0.003283	1.93	3.957	0.893	0.842	0.018845	0.017768
1.42	1.742	0.975	0.183	0.016732	0.003141	1.96	3.914	0.892	0.849	0.018053	0.017183
1.45	1.94	0.979	0.184	0.017945	0.003373	1.99	3.873	0.892	0.856	0.017330	0.016630
1.48	3.71	0.884	0.167	0.029743	0.005619	2.02	3.833	0.892	0.861	0.016645	0.016067
1.51	3.892	0.887	0.17	0.030076	0.005764	2.05	3.812	0.892	0.866	0.016073	0.015604

E (eV)	$\Phi \times 10^{17}$ ( $\text{cm}^2 \cdot \text{s}^{-1} \cdot \mu\text{m}^{-1}$ )	(1-R)Srp (CISE)	(1-R)Srp (CIS)	Jrg (CISE) ( $\text{A} \cdot \text{cm}^{-2} \cdot \text{eV}^{-1}$ )	Jrp (CIS) ( $\text{A} \cdot \text{cm}^{-2} \cdot \text{eV}^{-1}$ )	E (eV)	$\Phi \times 10^{17}$ ( $\text{cm}^2 \cdot \text{s}^{-1} \cdot \mu\text{m}^{-1}$ )	(1-R)Srp (CISE)	(1-R)Srp (CIS)	Jrg (CISE) ( $\text{A} \cdot \text{cm}^{-2} \cdot \text{eV}^{-1}$ )	Jrp (CIS) ( $\text{A} \cdot \text{cm}^{-2} \cdot \text{eV}^{-1}$ )
2.08	3.796	0.891	0.87	0.015530	0.015164	3.01	1.342	0.202	0.202	0.000594	0.000594
2.11	3.738	0.891	0.873	0.014861	0.014560	3.04	1.058	0.183	0.183	0.000416	0.000416
2.14	3.641	0.891	0.876	0.014072	0.013835	3.07	1.018	0.164	0.164	0.000352	0.000352
2.17	3.545	0.89	0.879	0.013310	0.013145	3.1	0.98	0.146	0.146	0.000296	0.000296
2.2	3.485	0.89	0.881	0.012730	0.012601	3.13	0.942	0.128	0.128	0.000244	0.000244
2.23	3.485	0.89	0.883	0.012390	0.012292	3.16	0.905	0.109	0.109	0.000196	0.000196
2.26	3.485	0.889	0.884	0.012050	0.011982	3.19	0.868	0.091	0.091	0.000154	0.000154
2.29	3.485	0.889	0.885	0.011736	0.011683	3.22	0.832	0.075	0.075	0.000120	0.000120
2.32	3.448	0.889	0.885	0.011313	0.011262	3.25	0.797	0.062	0.062	0.000093	0.000093
2.35	3.333	0.888	0.886	0.010646	0.010622	3.28	0.763	0.051	0.051	0.000072	0.000072
2.38	3.333	0.888	0.886	0.010380	0.010356	3.31	0.729	0.042	0.042	0.000056	0.000056
2.41	3.333	0.887	0.886	0.010111	0.010100	3.34	0.695	0.034	0.034	0.000042	0.000042
2.44	3.333	0.884	0.884	0.009831	0.009831	3.37	0.663	0.028	0.028	0.000032	0.000032
2.47	3.333	0.877	0.877	0.009518	0.009518	3.4	0.63	0.026	0.026	0.000028	0.000028
2.5	3.244	0.854	0.854	0.008805	0.008805	3.43	0.599	0.026	0.026	0.000026	0.000026
2.53	3.22	0.795	0.795	0.007944	0.007944	3.46	0.568	0.027	0.027	0.000025	0.000025
2.56	3.214	0.653	0.653	0.006362	0.006362	3.49	0.537	0.028	0.028	0.000025	0.000025
2.59	3.11	0.507	0.507	0.004669	0.004669	3.52	0.507	0.029	0.029	0.000024	0.000024
2.62	3.012	0.496	0.496	0.004323	0.004323	3.55	0.478	0.029	0.029	0.000022	0.000022
2.65	2.933	0.484	0.484	0.004016	0.004016	3.58	0.446	0.03	0.03	0.000021	0.000021
2.68	2.855	0.473	0.473	0.003735	0.003735	3.61	0.403	0.03	0.03	0.000018	0.000018
2.71	2.737	0.462	0.462	0.003420	0.003420	3.64	0.361	0.03	0.03	0.000016	0.000016
2.74	2.532	0.451	0.451	0.003022	0.003022	3.67	0.32	0.03	0.03	0.000014	0.000014
2.77	2.332	0.44	0.44	0.002656	0.002656	3.7	0.279	0.03	0.03	0.000012	0.000012
2.8	2.136	0.43	0.43	0.002327	0.002327	3.73	0.239	0.03	0.03	0.000010	0.000010
2.83	1.965	0.419	0.419	0.002042	0.002042	3.76	0.2	0.03	0.03	0.000008	0.000008
2.86	1.931	0.409	0.409	0.001918	0.001918	3.79	0.161	0.03	0.03	0.000007	0.000007
2.89	1.898	0.399	0.399	0.001801	0.001801	3.82	0.123	0.029	0.029	0.000005	0.000005
2.92	1.865	0.389	0.389	0.001690	0.001690	3.85	0.085	0.029	0.029	0.000003	0.000003
2.95	1.833	0.379	0.379	0.001586	0.001586	3.88	0.048	0.029	0.029	0.000002	0.000002
2.98	1.65	0.37	0.37	0.001366	0.001366						

## REFERENCES

1. S. M. Sze, "Physics of Semiconductor Devices", Wiley (1981), 51.
2. El Hadji Mamadou Keita, Abdoul Aziz Correa, Issa Faye, Chamsdine Sow, Cheikh Sene, Babacar Mbow. Short-Circuit Photocurrent Density Determination of Chalcopyrite Solar Cells and Study of Basic Parameters Under AM0, AM1, AM1.5 Spectra. Science Journal of Energy Engineering. Vol. 9, No. 4, 2021, pp. 79-89. doi: 10.11648/j.sjee.20210904.15
3. El Hadji Mamadou Keita, Fallou Mbaye, Bachirou Ndiaye, Chamsdine Sow, Cheikh Sene, Babacar Mbow. Optimizing Structures Based on Chalcopyrite Materials for Photovoltaic Applications. American Journal of Energy Engineering. Vol. 10, No. 3, 2022, pp. 53-67. doi: 10.11648/j.ajee.20221003.11
4. E. M. Keita, B. Ndiaye, M. Dia, Y. Tabar, C. Sene, B. Mbow, "Theoretical Study of Spectral Responses of Heterojunctions Based on  $\text{CuInSe}_2$  and  $\text{CuInS}_2$ " OAJ Materials and Devices, Vol 5#1, 0508 (2020) – DOI: 10.23647/ca.md20200508.
5. Henry Mathieu, Cours, "Physique des Semiconducteurs et des Composants Électroniques", 2001, 5e édition, DUNOD, p. 124-137
6. Bernard Sapoval, Claudine Hermann, "Physique des semi – conducteurs" copyright 1990, Ellipses, P.196
7. Michelle Schatzman, Cours et Exercices, Analyse Numérique, "Une Approche Mathématique", 2001, 2e édition, DUNOD, p.211.
8. R. Scheer, T. Walter, H.W. Schock, M.L. Fearheiley, H.J. Lewerenz, " $\text{CuInS}_2$  based thin film solar cell with 10.2% efficiency", Appl. Phys. Lett. 63 (1993) 3294.
9. R.A. Mickelsen, W.S. Chen, "High photocurrent polycrystalline thin-film  $\text{CdS/CuInSe}_2$  solar cell<sup>a</sup> ", Appl. Phys. Lett. 36 (1980) 371.

10. P.J. Dale, A.P. Samantilleke, G. Zoppi, I. Forbes, L.M. Peter, "Characterization of CuInSe<sub>2</sub> material and devices: comparison of thermal and electrochemically prepared absorber layers", J. Phys. D: Appl. Phys. 41 (2008) 085105.
11. Alain Ricaud, "Photopiles Solaires", De la physique de la conversion photovoltaïque aux filières, matériaux et procédés. 1997, 1e édition, Presses polytechniques et universitaires romandes, p.40.
12. Subba Ramaiah Kodigala, "Cu(In<sub>1-x</sub>Ga<sub>x</sub>)Se<sub>2</sub> based thin solar cells", 2010, Volume 35, Academic Press, ELSEVIER. Inc.
13. E. M. Keita, B. Mbow, C. Sene, " Perovskites and other framework structure crystalline materials", chap No 22: Framework structure materials in photovoltaics based on perovskites 3D", OAJ Materials and Devices, vol 5 (2), (Coll. Acad. 2021), p. 637-708. DOI: 10.23647/ca.md20201511.

**Important:** Articles are published under the responsibility of authors, in particular concerning the respect of copyrights. Readers are aware that the contents of published articles may involve hazardous experiments if reproduced; the reproduction of experimental procedures described in articles is under the responsibility of readers and their own analysis of potential danger.

### Reprint freely distributable – Open access article

**Materials and Devices is an Open Access journal** which publishes original, and **peer-reviewed** papers accessible only via internet, freely for all. Your published article can be freely downloaded, and self archiving of your paper is allowed and encouraged!

We apply « **the principles of transparency and best practice in scholarly publishing** » as defined by the Committee on Publication Ethics (COPE), the Directory of Open Access Journals (DOAJ), and the Open Access Scholarly Publishers Organization (OASPA). The journal has thus been worked out in such a way as complying with the requirements issued by OASPA and DOAJ in order to apply to these organizations soon.



**Copyright** on any article in Materials and Devices is retained by the author(s) under the Creative Commons (Attribution-NonCommercial-NoDerivatives 4.0 International (CC BY-NC-ND 4.0)), which is favourable to authors.

**Aims and Scope of the journal :** the topics covered by the journal are wide, Materials and Devices aims at publishing papers on all aspects related to materials (including experimental techniques and methods), and devices in a wide sense provided they integrate specific materials. Works in relation with sustainable development are welcome. The journal publishes several types of papers : A: regular papers, L : short papers, R : review papers, T : technical papers, Ur : Unexpected and « negative » results, Conf: conference papers.

(see details in the site of the journal: <http://materialsanddevices.co-ac.com>)

We want to maintain Materials and Devices Open Access and free of charge thanks to volunteerism, the journal is managed by scientists for science! You are welcome if you desire to join the team!

**Advertising in our pages helps us!** Companies selling scientific equipments and technologies are particularly relevant for ads in several places to inform about their products (in article pages as below, journal site, published volumes pages, ...). Corporate sponsorship is also welcome!

**Feel free to contact us!** [contact@co-ac.com](mailto:contact@co-ac.com)